Journal of Thermal Analysis and Calorimetry, Vol. 69 (2002) 909–917

CHARACTERIZATION OF PHASE TRANSITION OF $Ba_{2-x}Sr_xIn_2O_5$ BY THERMAL ANALYSIS AND HIGH TEMPERATURE X-RAY DIFFRACTION

T. Hashimoto, M. Yoshinaga, Y. Ueda, K. Komazaki, K. Asaoka and S. Wang*

Department of Applied Physics, College of Humanities and Sciences, Nihon University, 3-25-40 Sakurajousui, Setagaya-ku, Tokyo 156-8550, Japan

Abstract

The phase transitions of $Ba_{2-x}Sr_xIn_2O_5$ were investigated with various thermal analyses and high-temperature X-ray diffraction. It was clarified that crystal structure of $Ba_{2-x}Sr_xIn_2O_5$ with x=0.0~0.4 varies from brownmillerite through distorted perovskite to another distorted perovskite with increase of temperature. The phase transition from brownmillerite to distorted perovskite was revealed to be first order, whereas transition from distorted perovskite to another one was second order. The specimen with $x \geq 0.5$ showed only one first order phase transition from brownmillerite to distorted perovskite. The phase diagram of $Ba_{2-x}Sr_xIn_2O_5$ was established and existence of tricritical point at ~1100°C with x=0.4~0.5 was suggested.

Keywords: $Ba_{2-x}Sr_xIn_2O_5$, dilatometry, high-temperature X-ray diffraction, phase diagram, quantitative DTA, structural phase transition, TG-DTA

Introduction

It was reported that oxide-ion conductivity of $Ba_2In_2O_5$ increased drastically by the order of about 1.5 at ~910°C and that its conductivity in the temperature range more than ~910°C was larger than that of stabilized ZrO_2, frequently employed as an electrolyte of solid oxide fuel cells and O_2 gas sensor [1]. This abrupt increase of oxide-ion conductivity was attributed to the structural phase transition. It was reported that the crystal structure of $Ba_2In_2O_5$ was brownmillerite with ordered arrangement of oxide-ion vacancy and ideal cubic perovskite with random distribution of oxide-ion vacancy below and above ~910°C, respectively [2, 3]. Supposed was that the high oxide-ion mobility of $Ba_2In_2O_5$ above ~910°C was due to the random distribution of oxide-ion vacancy. Attempts to stabilize high temperature phase to room temperature, such as partial substitution of other cations for Ba and/or In site, have been carried out for exploration of new oxide-ion conductor. It was reported that the phase transition temperature increased with partial substi-

* Author for correspondence: E-mail: takuya@chs.nihon-u.ac.jp

1418–2874/2002/ $ 5.00

Akadémiai Kiadó, Budapest
Kluwer Academic Publishers, Dordrecht

tution of Sr^{2+} for Ba^{2+} site, whereas it decreased with substitution of Ga^{3+} for In^{3+} site [4–6]. Kakinuma *et al*. reported that they succeeded in stabilization of high temperature phase with high oxide-ion conductivity with simultaneous partial substitution of La^{3+} and Sr^{2+} for Ba^{2+} site in $Ba_2In_2O_5$ system [7].

Recently, we have carried out dilatometry, TG-DTA, quantitative DTA and high-temperature X-ray diffraction of $Ba_2In_2O_5$, resulting in denial of so far reported crystal structure and phase transition [8, 9]. It has been clarified that there exists the second order phase transition at ~1070°C in addition to the first order phase transition at ~910°C, showing agreement with the result of ^{17}O-NMR reported by Adler and co-workers [10]. Also it has been revealed by using X-ray diffraction with high sensitivity that the crystal structure of $Ba_2In_2O_5$ above ~910°C is not ideal cubic perovskite but distorted one and that the crystal structure above ~1070°C is another distorted perovskite. This indicated that the phase transition and crystal structure of cation substituted $Ba_2In_2O_5$ should be reexamined.

In this study, crystal structures and phase transitions of $Ba_{2-x}Sr_xIn_2O_5$ have been investigated by using dilatometry, TG-DTA, quantitative DTA and high-temperature X-ray diffraction with high sensitivity. Phase diagram of $Ba_{2-x}Sr_xIn_2O_5$ whose parameters are temperature and Sr content, x, has been established. By using variation of enthalpy at the first order phase transition, ΔH, observed with quantitative DTA, distribution of oxide-ion vacancy in high temperature phase has been discussed.

Experimental

$Ba_{2-x}Sr_xIn_2O_5$ (x=0.0~0.6) ceramic specimens were prepared by solid-state reaction method. Nominal amounts of powdery $BaCO_3$ (99.9%), $SrCO_3$ (99.9%) and In_2O_3 (99.9%) were mixed in ethanol. Prior to the mixing, all powders were dried at 100°C for more than 24 h. The mixture was calcined at 800°C for more than 24 h in air. The calcined powder was pressed into pellet with 20 mm diameter and sintered at 1400°C for 17 h in air followed by cooling at a rate of 200°C h^{-1}. The powder X-ray diffraction measurement revealed that all sample had single-phase brownmillerite orthorhombic structure. The molar volume of $Ba_{2-x}Sr_xIn_2O_5$ decreased monotonically with Sr content, indicating that Sr substituted successfully for Ba site.

The behavior of thermal expansion of sintered $Ba_{2-x}Sr_xIn_2O_5$ (x=0.0~0.6) was analyzed using dilatometry (Rigaku Co., Ltd.: TMA8310). The rectangular specimens with ~11×~4×~4 mm size and ~86% of the ideal density were cut from the pellet and employed for the measurements. All the measurements were performed under static air at a heating and a cooling rate of 10°C min^{-1} using Al_2O_3 as a reference rod and push rod. TG-DTA measurements (Rigaku Co., Ltd.: TG8120) were carried out on ~25 mg powder specimens under static air with heating rate of 10°C min^{-1} to determine the phase transition temperature of $Ba_{2-x}Sr_xIn_2O_5$. Al_2O_3 and Pt were used as reference and material for pan, respectively. The quantitative DTA measurements (Rigaku Co., Ltd.: DSC8270) on powder specimens were performed under static air to estimate the temperature, variation of enthalpy (ΔH), variation of entropy (ΔS) and

variation of specific heat capacity (ΔC_p) of the structural phase transition. The heating rate was 10°C min^{-1}. The mass of the specimen, reference and pan were the same as TG-DTA measurements.

The X-ray diffraction patterns of $Ba_{2-x}Sr_xIn_2O_5$ at temperatures of 900~1200°C were obtained by using Rigaku RINT-2500 (CuK_α: 50 kV- 250 mA). All the measurements were carried out under static air.

Results and discussion

Phase diagram of $Ba_{2-x}Sr_xIn_2O_5$ obtained with dilatometry

Figure 1 shows thermal expansion behavior of $Ba_{1.6}Sr_{0.4}In_2O_5$. Discrete shrinkage corresponding to the first order structural phase transition was observed at 1060°C by heating procedure, whereas another phase transition with second order represented by variation of slope was also observed at 1100°C by cooling procedure. Since the second order phase transition was not observed at heating procedure probably due to low kinetics of the first order phase transition [9], dilatometry measured at cooling procedure was employed to establish phase diagram of $Ba_{2-x}Sr_xIn_2O_5$ depending on temperature and Sr content, x.

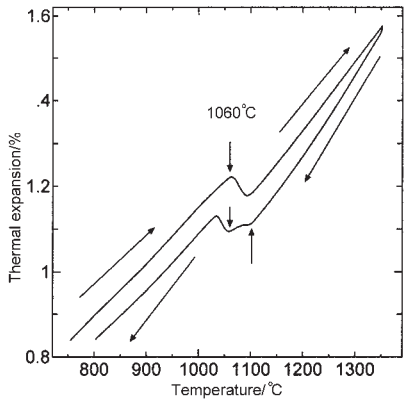

Fig. 1 Thermal expansion behavior of $Ba_{1.6}Sr_{0.4}In_2O_5$. At heating procedure, only one phase transition at 1060°C was observed whereas two kinds of phase transitions were observed at cooling procedure

Figure 2 shows temperature dependence of thermal expansion of $Ba_{2-x}Sr_xIn_2O_5$ (x=0.0~0.6) obtained at a cooling rate of 10°C min^{-1}. Temperatures for the first order phase transition and the second order one are depicted by arrow with upper direction and one with lower direction, respectively. For the specimens with x=0.0~0.4, two kinds of phase transition were observed. With increase of Sr content, temperature for the both phase transition increased and difference of the two kinds of phase transition

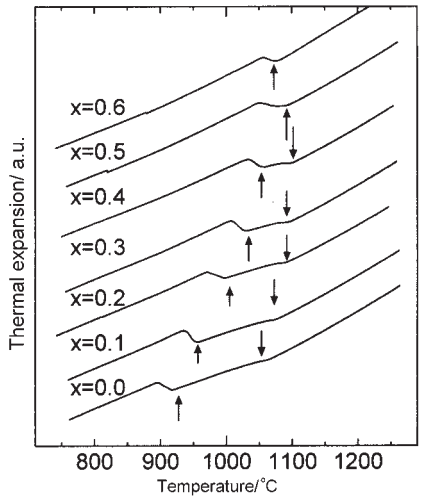

Fig. 2 Thermal expansion behavior of $Ba_{2-x}Sr_xIn_2O_5$ measured at a cooling rate of 10°C min^{-1}. ↑ – First order phase transition; ↓ – Second order phase transition

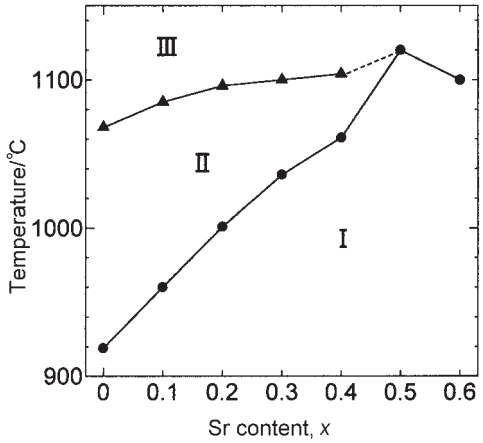

Fig. 3 Phase diagram of $Ba_{2-x}Sr_xIn_2O_5$. ● – First order phase transition ; ▲ – Second order phase transition

temperatures decreased. For the specimens with x=0.5 and 0.6, only the first order phase transition was observed and the second order one disappeared.

Figure 3 shows diagram of three $Ba_{2-x}Sr_xIn_2O_5$ (x=0.0∼0.6) phases, denoted as I, II and III, obtained with the result depicted in Fig. 2. With the increase of Sr content, temperature range in which phase II is stable became narrower. Existence of tricritical point for the specimen with x=0.4∼0.5 at ~1100°C was suggested.

High temperature X-ray diffraction of $Ba_{2-x}Sr_xIn_2O_5$

Three $Ba_2In_2O_5$ phases could be distinguished by X-ray diffraction at high temperatures. It was concluded that the phase I, II and III of $Ba_2In_2O_5$ were brownmillerite, distorted perovskite and another distorted perovskite, respectively [8, 9]. In this study, three phases of $Ba_{2-x}Sr_xIn_2O_5$ have been analyzed by X-ray diffraction at high temperatures. Figure 4 shows X-ray diffraction patterns of $Ba_{1.8}Sr_{0.2}In_2O_5$ at 980, 1080 and 1200°C at which the stable phase is I, II and III, respectively, according to the phase diagram shown in Fig. 3. All peaks of X-ray diffraction pattern at 980°C could be indexed as orthorhombic brownmillerite structure. Three peaks with relatively high intensity at 2θ=~29.4°, ~42.1°, and ~52.2° in X-ray diffraction pattern at 1080°C could be indexed as 110, 200 and 211 peak, respectively, assuming an ideal cubic perovskite structure. However, those represented by ○ or • could not be indexed as ideal cubic perovskite, indicating that the crystal structure of phase II is distorted perovskite. Since the X-ray diffraction pattern at 1200°C can be explained on the basis that diffraction peaks represented by • at 1080°C disappear whereas those represented by ○ remain, it is speculated that the difference of crystal structure between phase II and III can be ascribed to a slight deviation of atomic position. Thus clarified crystal structure of phase I, II, and III of $Ba_{1.8}Sr_{0.2}In_2O_5$ showed agreement with those of $Ba_2In_2O_5$ [8, 9].

Figure 5 shows X-ray diffraction patterns at $Ba_{1.5}Sr_{0.5}In_2O_5$ at 1050 and 1200°C at which the stable phase is I and III, respectively. All peaks of X-ray diffraction pattern at 1050°C could be indexed as orthorhombic brownmillerite structure. X-ray diffraction pattern at 1200°C could not be identified as brownmillerite structure, show-

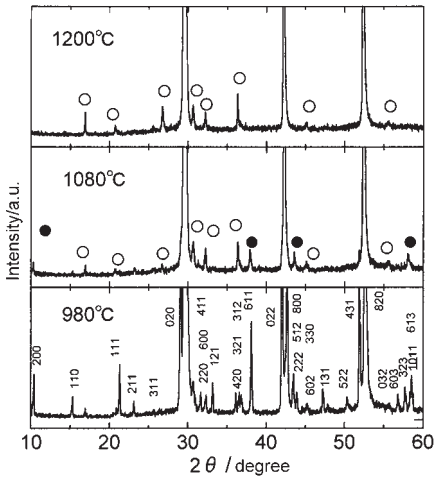

Fig. 4 X-ray diffraction patterns of $Ba_{1.8}Sr_{0.2}In_2O_5$ at 980, 1080 and 1200°C. Diffraction pattern at 980°C could be indexed as orthorhombic brownmillerite structure. Peaks, which cannot be indexed assuming ideal cubic perovskite structure, are represented by ○ or • in diffraction pattern at 1080°C. Peaks represented by ○ remain in diffraction pattern at 1200°C, whereas those depicted by • disappear

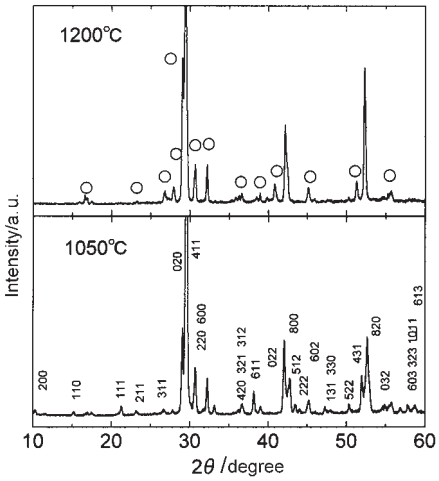

Fig. 5 X-ray diffraction patterns of $Ba_{1.5}Sr_{0.5}In_2O_5$ at 1050 and 1200°C. Diffraction pattern at 1050°C could be indexed as orthorhombic brownmillerite structure. Peaks, which cannot be indexed assuming ideal cubic perovskite structure, are represented by ○ in diffraction pattern at 1200°C

ing agreement with the phase transition observed with dilatometry. In addition to the three peaks with high intensity at 2θ=~29.5, ~42.2 and ~52.3° which could be indexed as cubic perovskite, peaks represented by ○ were observed. These ○ peaks indicated that the crystal structure of $Ba_{1.5}Sr_{0.5}In_2O_5$ at 1200°C was distorted perovskite.

Figure 6 shows X-ray diffraction patterns of $Ba_{2-x}Sr_xIn_2O_5$ with x=0.0, 0.2 and 0.5 at 1200°C. Irrespective x, three peaks with relatively high intensity which could be indexed assuming ideal cubic perovskite and peaks represented by ○ and arrows which could not be explained as ideal cubic perovskite were observed. Overall, there observed was little difference among these three patterns, indicating that the same phase appeared at 1200°C irrespective of Sr content, showing agreement with the phase diagram shown in Fig. 3. The peaks represented by ○ and arrows could be explained as derived ones from distortion from ideal cubic perovskite structure. The intensity of the peaks indicated by arrows increased with increase of x probably because difference of tolerance factor of $Ba_{2-x}Sr_xIn_2O_5$ perovskite structure from 1 increased with increase of Sr content [6].

Quantitative DTA measurements of $Ba_{2-x}Sr_xIn_2O_5$ (x=0.0~0.6)

In order to analyze the thermodynamic character of the observed phase transitions, quantitative DTA of $Ba_{2-x}Sr_xIn_2O_5$ (x=0.0～0.6) were measured. Figure 7 shows quantitative DTA curves of the specimens with x=0.0, 0.2 and 0.4. Endothermic peak at 905°C and base-line shift at 1070°C corresponding to the first order phase transition and second order one, respectively, were observed in the quantitative DTA curve of $Ba_2In_2O_5$. Also in the quantitative DTA curves of the specimens with x=0.2 and 0.4,

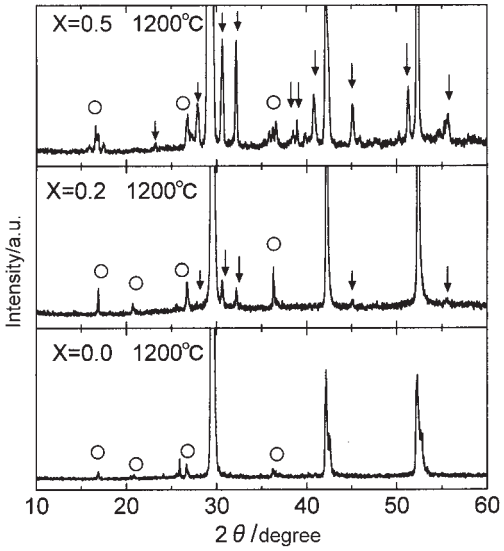

Fig. 6 X-ray diffraction patterns of $Ba_{2-x}Sr_xIn_2O_5$ at 1200°C. ○ – peaks common to the three patterns ↓ – peaks whose intensity increased with x

endothermic peak and base-line shift were observed although the phase transition temperature varied by Sr content, x. TG measurements revealed that there existed no mass variation in the temperature range 850～1300°C, indicating that the phase transition did not involve generation of oxide-ion vacancy nor evaporation of In. The phase transition temperatures obtained by quantitative DTA showed agreement with those obtained by dilatometry.

Characterization of the first order phase transition of $Ba_{2-x}Sr_xIn_2O_5$ from the viewpoint of variation of crystal structure and thermodynamic function

High oxide-ion conductivity of $Ba_2In_2O_5$ above ~910°C was ascribed to the randomly distributed oxide-ion vacancy in ideal cubic perovskite structure in the preceding studies [1–7]. Since it has been clarified that high temperature phase of $Ba_{2-x}Sr_xIn_2O_5$ is not ideal cubic perovskite but distorted one in this study, it should be reexamined that the oxide-ion distribution in high temperature $Ba_{2-x}Sr_xIn_2O_5$ phase is random or not. From the measurement of variation of enthalpy, ΔH, at the first order phase transition, hypothesis on oxide-ion distribution in $Ba_{2-x}Sr_xIn_2O_5$ can be examined.

In the brownmillerite structure, number of oxide-ion site and oxide-ion vacancy site is 5 and 1 per one molecule, respectively. If the oxide-ion and oxide-ion vacancy mix randomly at the first order phase transition, variation of configuration entropy, ΔS_{conf} is represented by follows [11].

$$\Delta S_{conf} = -R(X_a \ln X_a + X_b \ln X_b) = 3.74 \text{ J mol}^{-1} \text{ K}^{-1}$$

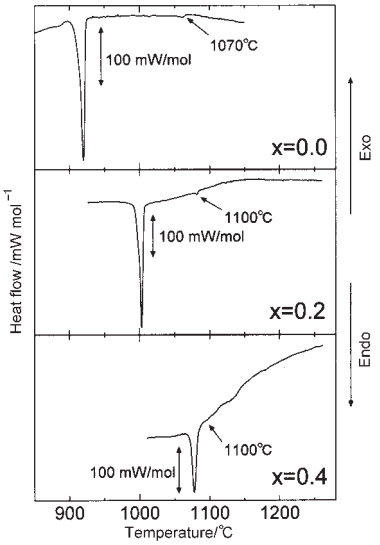

Fig. 7 Quantitative DTA curves of $Ba_{2-x}Sr_xIn_2O_5$ with x=0.0, 0.2 and 0.4. Two kinds of phase transitions were observed in each specimen

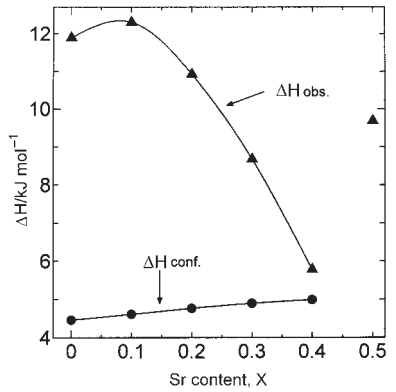

Fig. 8 ΔH of $Ba_{2-x}Sr_xIn_2O_5$ at the first order phase transition temperature. ▲ – observed ΔH with quantitative DTA (ΔH_{obs}) ● – calculated ΔH to make the oxide-ion distribution perfectly random (ΔH_{conf})

Here, X_a and X_b denotes probability of existence of oxide-ion and that of oxide-ion vacancy *vs*. all anion sites and is equal to 5/6 and 1/6, respectively. Variation of configuration enthalpy, ΔH_{conf}, is a product of phase transition temperature and ΔS_{conf}. Figure 8 shows ΔH_{conf} thus calculated. Also shown in Fig. 8 are ΔH_{obs} obtained by using the endothermic peak area of quantitative DTA curves of $Ba_{2-x}Sr_xIn_2O_5$. ΔH_{obs} are larger than ΔH_{conf} for all the specimens examined, indicating that enough heat quantity is absorbed in order to make the distribution of oxide-ion vacancy perfectly random at the first order phase transition.

Conclusions

Two kinds of phase transitions were observed in $Ba_{2-x}Sr_xIn_2O_5$ system, one was the first order and the other the second order, by using dilatometry, TG-DTA, quantitative DTA and high-temperature X-ray diffraction. The crystal structures of $Ba_{2-x}Sr_xIn_2O_5$ at high temperatures were revealed to be not the ideal cubic perovskite but distorted ones. Phase diagram of $Ba_{2-x}Sr_xIn_2O_5$ three phases was established and existence of tricritical point was suggested at ~1100°C for the specimen with x=0.4~0.5. ΔH at the first order phase transition observed by quantitative DTA was large enough to make the oxide-ion vacancy distribution perfectly random.

* * *

This study was partly supported by a Grant from the Ministry of Education, Science, Sports and Culture to promote advanced scientific research.

References

1 J. B. Goodenough, A. Manthiram, P. Paranthaman and Y. S. Zhen, Solid State Ionics, 52 (1992) 105.
2 H. Kobayashi, K. Nakamura, T. Mori, H. Yamamura and T. Mitamura, Denki Kagaku, 64 (1996) 683.
3 Y. Uchimoto, M. Kinuhata, H. Takagi, T. Yao, T. Inagaki and H. Yoshida, SOFC-VII, The Electrochemical Society, Pennington NJ 1999, p. 317.
4 Y. Yao, Y. Uchimoto, M. Kinuhata, T. Inagaki and H. Yoshida, Solid State Ionics, 132 (2000) 189.
5 C. A. J. Fisher, B. Derby and R. J. Brook, Br. Ceram. Proc., 56 (1996) 25.
6 H. Yamamura, Y. Yamada, T. Mori and T. Atake, Solid State Ionics, 108 (2000) 377.
7 K. Kakinuma, H. Yamamura, H. Haneda and T. Atake, Solid State Ionics, 140 (2001) 301.
8 T. Hashimoto, K. Asaoka, K. Komazaki, Y. Ueda and M. Yoshinaga, Proc. of the 4th Int'l Symp. on Ionic and Mixed Conducting Ceramics, The Electrochemical Society, Pennington NJ 2001, in press.
9 T. Hashimoto, Y. Ueda, M. Yoshinaga, K. Komazaki, K. Asaoka and S. Wang, J. Electrochem. Soc., in press.
10 S. B. Adler, J. A. Reimer, J. Baltisberger and U. Werner, J. Amer. Chem. Soc., 116 (1994) 675.
11 R. A. Swallin, Thermodynamics of Solids, Wiley, New York 1962.